Polymer Degradation and Stability 128 (2016) 1–7

Contents lists available at ScienceDirect

Polymer Degradation and Stability

journal homepage: www.elsevier.com/locate/polydegstab

Effect of polymer branching on degradation during inkjet printing

Joseph S.R. Wheeler [a], Amélie Longpré [b], Daniel Sells [d], Daryl McManus [a], Steven Lancaster [c], Stuart W. Reynolds [c], Stephen G. Yeates [a, *]

[a] Organic Materials Innovation Centre, School of Chemistry, University of Manchester, Manchester, M13 9PL, United Kingdom
[b] ITECH Textile and Chemical Institute, 87 Mouilles Ecully Way, Mouilles Ecully, Cedex, Lyon, France
[c] Domino UK Ltd, Trafalgar Way, Bar Hill, Cambridge, CB23 8TU, United Kingdom
[d] School of Chemistry, University of Manchester, United Kingdom

ARTICLE INFO

Article history:
Received 25 January 2016
Received in revised form
17 February 2016
Accepted 22 February 2016
Available online 26 February 2016

Keywords:
Inkjet
Hyperbranched
EPR
Polymer
Degradation

ABSTRACT

In this paper we demonstrate the potential of high molecular weight hyperbranched methacrylate polymers for inkjet printing. Using the Strathclyde method, a series of hyperbranched poly (methylmethacrylate) polymers of increasing branch density were prepared. All hyperbranched polymers show both a significantly greater maximum printable concentration compared to equivalent linear polymers with implications for faster print speed. Increasing chain branching above a critical value across the molecular weight distribution was found to result in suppression of molecular weight degradation. This resistance to molecular degradation is because the longest chain segment being much smaller, such that upon jetting the polymer rapidly retains its thermodynamically stable Gaussian coil conformation and the full force of the constrictional flow in the print head is not passed on to the polymer and degradation is supressed. We further go on to show using Electron Paramagnetic Resonance that degradation occurs via a free radical chain scission mechanism.

1. Introduction

Inkjet printing has developed as an important technology for the controlled deposition of functional fluids in applications as diverse as graphics, textiles, biological printing and digital fabrication [1–5]. Two technologies currently dominate the drop generation process, drop on demand (DOD), and continuous inkjet (CIJ). DOD involves the ejection of fluid through a constricted nozzle with a diameter between 10 and 80 μm, through the application of an appropriate pressure wave [6,7]. In comparison CIJ printing consists of a stream of ink passing through a nozzle which breaks up into droplets through the application of a piezo generated continuous acoustic wave. Both approaches have associated formulation challenges and requirements which make them more or less suitable for specific applications [6,7].

The need to deposit soluble functional polymers is important in a number of technology areas including photonics, electronics and biologics [8–12]. High molecular weight and/or high concentration are often desirable for high speed single pass printing and/or to produce a mechanically robust film without the need for post curing technologies. It has long been recognised however that the addition of small amounts of polymer to an ink formulation can have a large and deleterious effect on the print performance with both polymer–solvent interaction, polymer concentration and molecular mass influencing drop ejection and breakup, and leading to formulation compromises [13–15].

At the very high elongational strain rates (γ) experienced in both DOD and CIJ printing, the polymer chain is perturbed from its thermodynamically stable Gaussian coil to a chain extended conformation. If the relaxation time of the polymer from the chain extended state (λ) to its thermodynamically stable Gaussian coil conformation is sufficiently long then the viscoelasticity of the fluid under drop formation and ejection will be strongly influenced [13–15]. The criteria for extended chain persistence is given by the critical Weissenberg number ($Wi = \lambda\gamma_{crit}$) [16–19], and when $Wi > 0.5$ the majority of a polymer sample will be in the chain extended state. In such studies, λ is typically given by the Zimm relaxation time (λz) since this defines the longest possible chain relaxation of a polydisperse sample [16–19].

It is well documented that above γ_{crit}, there is a further critical strain rate γ_{deg}, which will cause the polymer chain to undergo chain scission; provided it exceeds a critical residence time within

* Corresponding author.
E-mail address: stephen.yeates@Manchester.ac.uk (S.G. Yeates).

http://dx.doi.org/10.1016/j.polymdegradstab.2016.02.012

the high shear environment. As polymer molecular weight increases γ_{crit} and γ_{deg} converge and at a critical molecular weight of *ca.* 5×10^6 Da it is not possible for a polymer to undergo its coil stretch transition without chain scission, with monodisperse polymers being found to break centro-symmetrically and polydisperse samples randomly under elongational flow [16–19].

We have recently reported that the degradation of a linear polymer can occur in both CIJ and DOD if certain criteria are met with regards to molecular weight value, molecular weight distribution, concentration and nozzle geometry [20–22]. Subsequent simulation work supported the assertion that degradation is not due to extensional flow in the ligament after the drop is ejected but rather the high strain rate and constrictional flow in the nozzle itself [23]. However until now we have not considered the role of polymer structure with respect to branching. It is well documented that branching can increase solubility and allow for the formulation of high concentration and low viscosity fluids when compared to those formulations prepared with analogous linear counterparts [24,25]. To date the only consideration of the role of polymer branching in high molecular weight polymers in an inkjet context is by De Gans et al., who showed that the jetting performance and ligament formation properties of 3 and 5 armed star polymers was improved when compared to linear polymers [26].

In this paper we show for the first time hyperbranched polymers, prepared using the experimentally straightforward Strathclyde method [27,28], are capable of being inkjet printed at significantly greater volume fraction than their equivalent analogous linear counterparts with the potentially desirable film forming attributes that high molecular weigh polymers offer, and go on to demonstrate significantly improved resistance to flow induced molecular weight degradation. As a consequence of the greater maximum printable polymer concentration and the higher density of chain ends we are able to provide greater insight into the degradation mechanism using Electron Paramagnetic Resonance (EPR) studies.

2. Experimental

2.1. Materials

All solvents, linear atactic poly(methyl methacrylate) (PMMA; $M_w = 90$ kDa, Pdi = 2; $M_w = 310$ kDa, Pdi = 2.8; $M_w = 468$ kDa, Pdi = 3.3) were obtained from Sigma Aldrich UK and used as received. The solutions prepared with these polymers are referred to as PMMA 90 kDa, PMMA 310 kDa and PMMA 468 kDa throughout this publication. Three hyperbranched PMMA polymers having low, medium and high branching (LB, MB and HB respectively) were synthesised according to the Strathclyde method [27–29] details of which are given in S1. N-tertiary-butyl nitrone (PBN) was obtained from Sigma Aldrich (98%) and used as received. Polymer solutions were prepared by mechanical stirring using a Janke and Kundel RW 20 at 35 °C for 3 h, and filtered using a Buchner funnel with Whatman Qualitative filter paper.

2.2. Instrumentation

Dynamic viscosity measurements were carried out with a Brookfield DVII + viscometer at a temperature of 25 °C (±0.2 °C). All samples were equilibrated in a temperature controlled water bath for 30 min. Intrinsic viscosity measurements were carried out using an Ubbelohde capillary viscometer; dilute solutions ranging from 0.3 to 1.5 g/dl were made up and equilibrated at a temperature of 25 °C (±0.2 °C) for 30 min. The flow time of these solutions through the capillary was measured and the intrinsic viscosity determined by plotting functions of the specific and relative viscosity against concentration and extrapolating to zero concentration.

Shear stability to ultrasound was carried out using a Missonix 300 ultrasonic probe. All sonication experiments were carried out in an ice water bath to prevent macro heating of the solution. 20 mL of polymer solution was placed in a round bottom flask and the probe submerged in the solution leaving a 5 cm gap between the probe and the bottom of the container. The solution was irradiated at a power between 27 and 33 W.

Drop on demand inkjet printing was carried out using a Dimatix DMP-2800 fitted with a waveform editor and a drop-watch camera system which allows manipulation of the electronic pulses to the piezo jetting device for optimisation of the drop characteristics as it is ejected from the nozzle [20]. CIJ experiments were carried out using a Domino A-Series+ with the printhead removed. This configuration was chosen as previous studies have shown that polymer degradation occurs in both the pump and filters and not the drop formation process itself [22].

Before molecular weight determination, the polymeric materials were precipitated from solution by addition of a large excess of ice cold petroleum ether (40–60 °C bpt) and dried in a vacuum oven. Molecular weights were measured using gel permeation chromatography (GPC) in tetrahydrofuran (THF) comprising a Viscotek GPCmax VE2001 solvent/sample module fitted with 2 × PL gel 10 μm Mixed-B and PLgel 500 Å columns, a Viscotek VE3580 RI and a VE 3240 UV/VIS multichannel detector. The flow rate was 1 mL/min and the system calibrated with low polydispersity PMMA standards in the range of 200 to 2.2×10^6 g/mol, with dodecane as flow marker. Samples were made up to a concentration of 1 mg/ml and pre-filtered using a Whatman 0.45 μm filter. GPC measurements were also performed on a Viscotek TDA305 system using a triple detection capability with a fitted refractometer, viscometer and MALS with methyl ethyl ketone (MEK) as the eluent. Samples were made up to a concentration of 1–5 mg/ml and pre-filtered using Millex 0.45 μm filters. In both GPC systems the columns were heated to 35 °C. A full description of the triple detection GPC methodology and experimental set up is given in S5.

Drop drying experiments were carried out by printing on glass substrates treated with concentrated sulphuric acid and cleaned with distilled water and acetone followed by drying in an oven at 100 °C for 15 min. The analysis of the dried drops was carried out using optical microscopy and atomic force microscopy (AFM).

EPR measurements were carried out using a Bruker EMX Micro X band Spectrometer. Polymer solutions containing PBN spin trap at a concentration of 0.1 M. Solutions were either sonicated or inkjet printing under ambient conditions and subsequently nitrogen purged, frozen in liquid N_2 and thawed prior to measurement.

3. Results and discussion

3.1. Polymer characterisation

The synthesis of the hyperbranched PMMA polymers was achieved using a one-step, 100 g scale solution polymerisation reaction based on the Strathclyde method, S1 [27–29]. The reaction is essentially a linear polymerisation doped with appropriate amounts of a multifunctional monomer, tripropylene glycol diacrylate (TPGDA) and chain transfer agent, dodecanethiol (DDT). The stoichiometric balance between monomer, multifunctional monomer and chain transfer agent is critical in determining whether the polymer maintains solubility throughout the reaction or gels with an insoluble cross-linked network. Ratios of monomer: chain transfer agent: multifunctional monomer and a molecular weight data of the hyperbranched PMMA polymers used in this study are given in Table 1.

Fig. 1a shows the molecular weight distribution of the three

Table 1
Physical properties of hyperbranched polymers used in the study.

Polymer code	MMA:TPGDA:DDT (mol:mol:mol)	M_n (kDa)	M_w (kDa)	a	[η] dL/g @ 25 °C
PMMA 468 kDa	100/0/0	140	468	0.69	0.77
LB	100/1.42/0.84	12	113	0.39	0.1
MB	100/1.78/0.86	26	360	0.38	0.17
HB	100/2.2/0.98	90	609	0.44	0.5

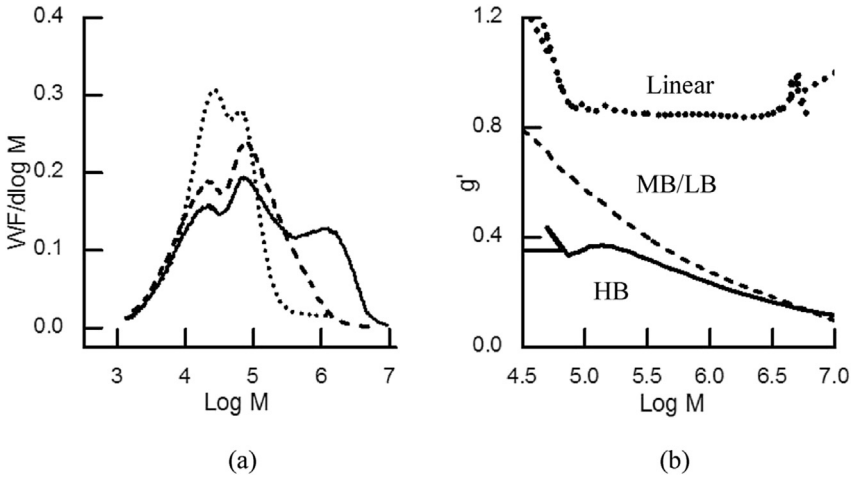

Fig. 1. (a) Molecular weight distributions of: HB (solid line), MB (dashed line) and (c) LB (dotted line); (b) branching frequency (g′) for linear PMMA 468 kDa (Dotted Line), LB and MB (dashed line) and HB (solid line).

hyperbranched polymers used in this study. The evolution of the distribution has previously been described and the emergence of "shoulders" in the molecular weight distribution (MWD) is commonly observed in branched polymers [29]. This is rationalised by the presence of multiple MWDs with equivalent radii of gyration due to the random nature of the free radical reaction used to synthesise these polymers; the macromolecules formed will contain a range of branching and molecular weights, which cannot be differentiated by chromatography [29]. Triple detection GPC measurements confirm the branched nature of the hyperbranched polymers when compared to linear PMMA, Fig. 1b. In all cases the Mark–Houwink *a*-values as determined in MEK are significantly lower for all three hyperbranched polymers compared with linear PMMA 310 kDa, $a = 0.4$ compared with $a = 0.69$, indicating a more compact structure and higher molecular density. Branching was calculated using a Zimm-Stockmeyer model first reported by Frechet and co-workers which relates the intrinsic viscosities of the branched fractions to that of the linear reference materials [30], with the highest molecular weight fractions for the hyperbranched polymers being the most highly branched through successive generation. As can be seen in Fig. 1b, HB being more highly branched compared with both LB and MB over the whole molecular weight range as evidenced by the lower branching ratio, g'. A full explanation of the branching calculations is given in S4.

Increasing molecular weight for linear PMMA in MEK from M_w of 90 kDa–468 kDa results in an increase intrinsic viscosity from 0.22 to 0.77 g/dl and a decrease in overlap concentration (c^*) from 5.2 to 2.9 g/dl [20]. In contrast LB, MB and HB all have significantly lower intrinsic viscosities ranging from 0.1 to 0.5 and c^* values up to 8.5 g/dL. This has consequences for the viscosity concentration profiles of hyperbranched polymers when compared to linear polymers.

3.2. Inkjet printing of hyperbranched polymers

It can be seen from Fig. 2a that the viscosity of hyperbranched polymer solutions is significantly lower than that of linear polymer formulations at comparable concentrations in MEK (a good solvent) at 25 °C. This is due to significantly lower chain overlap as a result of the compact conformations that hyperbranched polymers adopt in solution when compared to linear polymers of comparable molecular weight. This has consequences for the maximum concentration of hyperbranched polymers that are printable by inkjet methods. Viscosity is of particular importance for inkjet printing due to the constraints on the formulation of polymer containing fluids [34]. The lower intrinsic viscosity of the hyperbranched polymer when compared to linear samples of equivalent molecular weight results in a higher printable concentration for the former [31,32]. Hyperbranched polymers were found to be printable by DOD up to 8.5 g/dL without nozzle blockage or deterioration in print quality, compared with 2.9 g/dL for PMMA 468 kDa. Given the high molecular weight fraction above 5×10^5 Da, this is particularly striking as earlier work has shown that DOD jetting is not possible at $c/c^* > 0.5$ for $Mw > 5 \times 10^5$ Da for linear PMMA and PS in a good solvent [16,32]. The drop formation behaviour in all cases followed that previously observed for DOD [13]. At low polymer concentrations a leading drop would form with the ligament tail rupturing along the length into many satellite drops [16]. As the concentration increases the ligament breaks resulting in a single satellite drop and a single printing drop is produced from ligament recoil at high concentration [13]. Since HB has a significantly higher maximum printable concentration it shows a greater quantity of material deposited per drop, Fig. 2b, which has implications for any application which involves the deposition of large volumes of functional polymeric materials, eliminating the potential need for multiple print, dry, print protocols [33]. It should be noted that the coffee-ring effect is still present since a single solvent system was

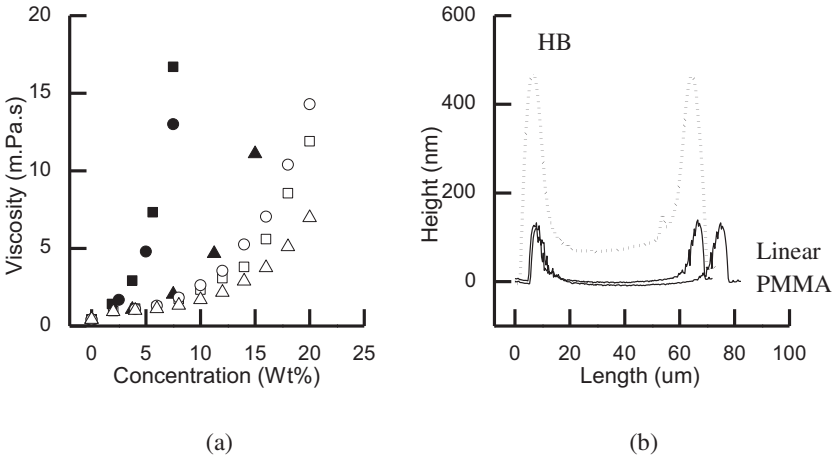

Fig. 2. (a) Viscosity versus concentration in MEK at 25 °C for PMMA 90 kDa (▲), PMMA 310 kDa (●), PMMA 468 kDa (■), LB (Δ), MB (○) and HB (□); (b) Overlayed AFM drop profiles of the dried drops of the maximum printable concentration formulation of PMMA 468 kDa, PMMA 90 kDa (solid lines) and HB (dotted lines) in MEK.

used and reformulation will be required to eliminate. The high printable concentration without nozzle blockages for the branched polymers is rationalised by the much shorter effective relaxation rates from the chain extended state (λ) to its thermodynamically stable Gaussian coil conformation. The longest linear chain segment in a hyperbranched polymer is much shorter than that of a linear polymer with a comparable molecular weight.

3.3. Molecular weight stability of hyperbranched and linear polymers upon ultrasonic treatment

It is well documented that exposure of polymeric material to ultrasound can result in irreversible molecular weight degradation as a consequence of the high shear gradients generated [34]. The observed degradation mode depends on the nature of the molecular weight distribution of the polymer: monodisperse polymers break centrosymetrically with the PDI converging on a value of 2 and the higher molecular weight fractions of a polydisperse material degrade preferentially leading to a random degradation mechanism for the overall sample. A rapid decrease in molecular weight was observed for the polydisperse PMMA 468 KDa in γ-butyrolactone with increasing sonication time, Fig. 3a. Degradation rate is highest at low concentration as cavitation is supressed in higher viscosity fluids [35,36].

In the case of MB and HB sonicated in xylene for a period of up to 10 min, Fig. 3b and c, it can be seen that molecular weight > 10^5 Da are degraded preferentially leaving a shear resistant bimodal distribution comprising the most highly branched, Fig. 1a. This suggests that the branched chain ends are being preferentially shaved leaving a branched central core, and hence the molecular weight distribution retains a bimodal distribution rather than a Gaussian distribution. Similar behaviour has been previously observed in the sonication of star polymers with the arms being removed from a central core [37].

3.4. Molecular weight degradation of branched materials in DOD and CIJ printing

The molecular weight distribution of the hyperbranched polymers and the linear reference of PMMA 468 kDa were evaluated before and after jetting from a DOD printhead at a reduced concentration of0.15 in the chosen solvent. This was achieved with a Dimatix DMP printer using an applied voltage of 40 V yielding a drop velocity of 6–10 ms^{-1} and a calculated shear rate of ca 400,000 s^{-1}. As expected in the context of the work of al-Alamry et al. [20] there is a reduction in molecular weight of a linear

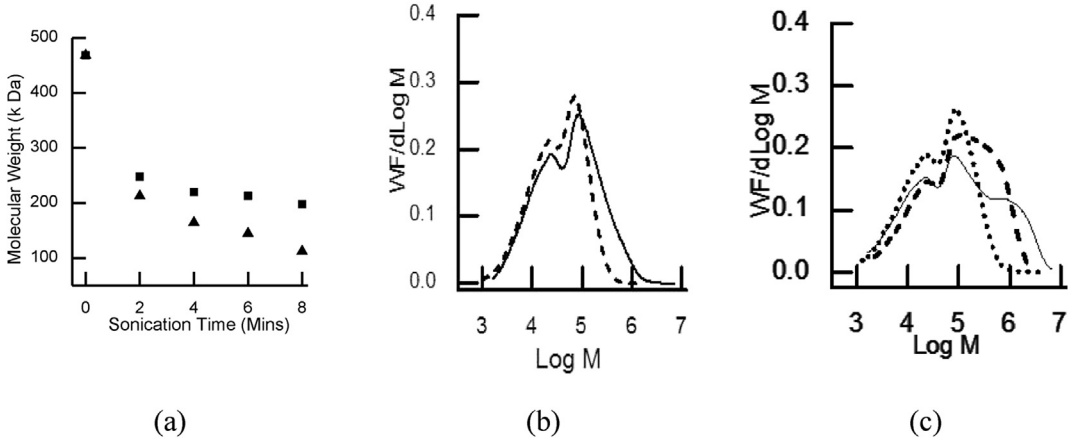

Fig. 3. Development of molecular weight after sonication: (a) PMMA 468 kDa after 8 min of sonication in γ-Butyrolactone. (■) $c/c^* = 1$. (▲) $c/c^* = 0.15$; (b) MB pre sonication (solid lines) and post (---) 10 min sonication in xylene at a c/c^* of 1; and (c) HB pre sonication (solid line) after 2 min of sonication (Dashed line) and after 10 min of sonication (dotted line) in xylene at a power of 33 W at a c/c^* of 1.

control PMMA 468 kDa in γ-butyrolactone, Fig. 4a. For both the low and medium branched samples LB and MB in xylene, Fig. 4b and c, reduction of the high molecular weight fraction and concomitant increase in the <500 kDa fraction was observed irrespective of polymer concentration with behaviour similar to that of linear polymer.

However when the degree of branching is increased further in sample HB in xylene, the molecular weight distribution is largely unaffected by the inkjet printing process, Fig. 4d apart from a small shaving of the highest molecular weight fractions, ca 10^7 kDa. Even though the overall polymer has a very high molecular weight, the shear resistance arises from the longest chain segment being much smaller, such that upon jetting the polymer rapidly retains its thermodynamically stable Gaussian coil conformation and the full force of the constrictional flow in the print head is not passed on to the polymer and degradation is supressed. Similar observations are seen in CIJ where a 15 g/dl solution of HB was recirculated through the pumps and filters of a Domino A-Series +, which have previously been shown to be the locus of polymer degradation [24]. Whilst some degradation in molecular weight was observed, the change in molecular weight distribution is significantly less than for a comparative linear samples, Fig. 5 a and b. HB maintains a significant fraction of its high molecular weight fraction which in the case of linear polymers are degraded after a comparable number of duty cycles, showing that the hyperbranched polymers can also withstand high shear environments for longer periods than comparable linear systems. Due to the increased concentration of polymer needed to formulate at the target c/c*, the solubility of the hyperbranched solution in the medium was of greater importance than the solvent viscosity.

3.5. Polymer degradation study using EPR

The hyperbranched polymers prepared for this study enable us for the first time to probe the mechanism of chain degradation under DOD print conditions because of the higher printable concentrations possible and the higher chain end density. It is well documented that degradation of linear polymers under sonication proceeds by a free radical mechanism, whilst it has been shown that some ladder type polymers degrade by a heterolytic mechanism [36–38]. Polymer solutions containing the spin trap PBN were exposed to a series of identified conditions, which were known to induce polymer degradation. In all cases toluene was chosen for its low dielectric constant and high boiling point.

Sonication of 4 g/dl PMMA 468 kDa with PBN, Fig. 6a, shows a large signal increase of quenched PBN under non-oxygen degassed conditions, with increasing signal intensity with both sonication time and power. When the same formulation was recirculated through the pumps and filters of a Domino CIJ printer for a single statistical pass a similar spin trap signal was similarly observed, Fig. 6b, indicative of homolytic covalent bond scission rather than polymer becoming trapped in filters or precipitating out due to

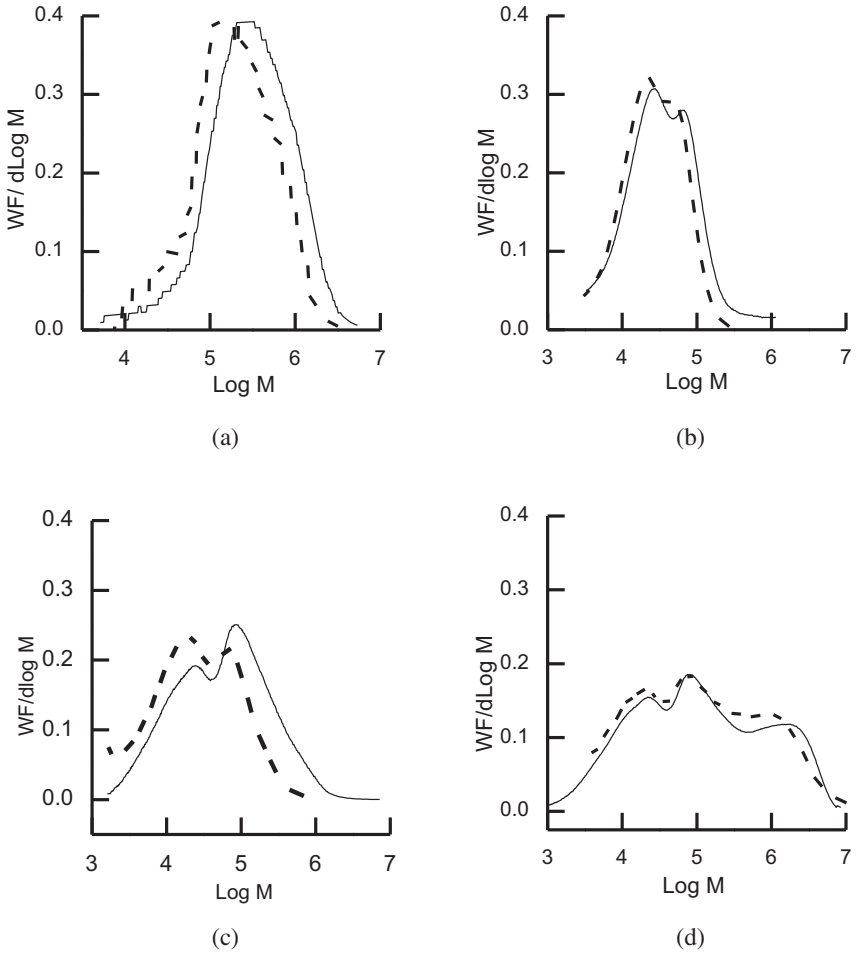

Fig. 4. Effect of branching on molecular weight stability during single pass DOD jetting at 40 V using a Dimatix DMP Printhead at 25 °C. before jetting (—), and after jetting (— —). (a) PMMA 468 kDa in γ-Butyrolactone at c/c* = 0.15; (b) LB, at c/c* = 0.15 in xylene; (c), MB at c/c* = 0.15 in xylene; (d) HB at c/c* = 0.15 in xylene.

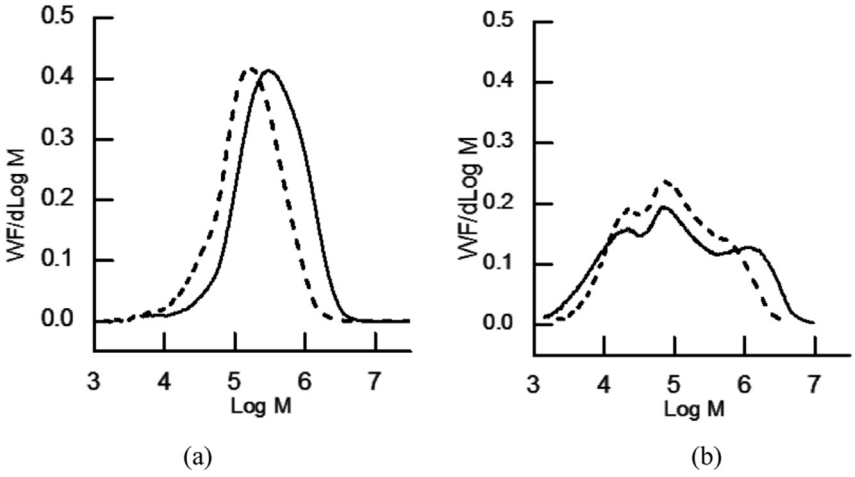

Fig. 5. The development of molecular weight after 250 h recirculation through the pumps and filters of a Domino A-Series +: (a) PMMA 468 kDa before (solid line) and after (dashed line); (b) HB before (solid line) and after (dashed line).

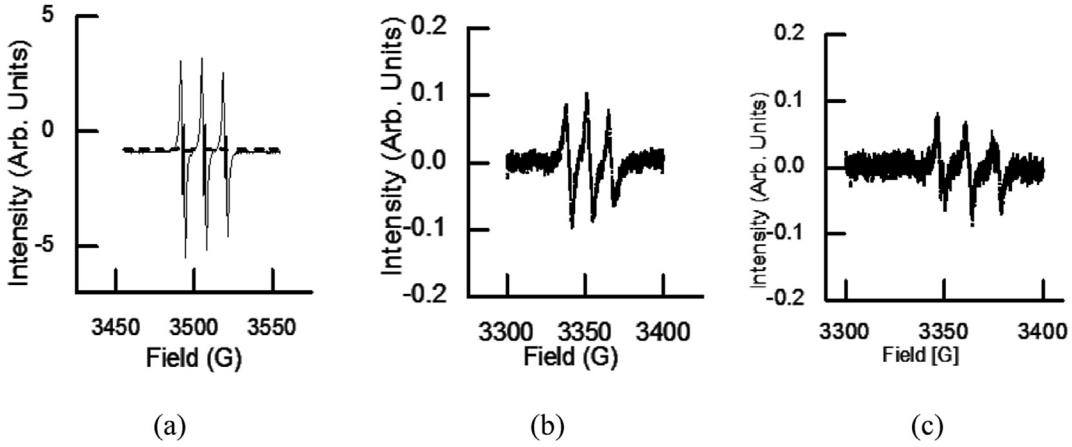

Fig. 6. Electron paramagnetic resonance (EPR) spectrum using N-tertiary-butyl nitrone (PBN) at 25 °C: (a) 4 g/dl PMMA 468 kDa in toluene after sonication for 8 min at a power of 33 W; (b) 4 g/dl PMMA 468 kDa in toluene after 250 h recirculation through the pumps and filters of a Domino A-Series +; and (c) 8.5 g/dl MB in toluene single pass through a Dimatix DMP printhead at 40 V.

strain induced crystallisation [21]. Extension to single pass DOD with this polymer was not possible due to a combination of a low print concentration and chain end density resulting in any spin trap signal being below the limit of detection.

A higher concentration and chain density was achieved for the hyperbranched sample of MB and this will lead to a greater susceptibility to degradation by jetting from a DOD printhead. We observed on single pass a detectable concentration of radical adduct, for MB, Fig. 6c, and confirms for the first time a free radical mechanism for polymer degradation in DOD inkjet printing.

4. Conclusion

We show that the viscosity of hyperbranched polymer solutions is significantly lower than that of linear polymer formulations at comparable concentrations in good solvent at 25 °C. This is due to significantly lower chain overlap as a result of the compact conformations that hyperbranched polymers adopt in solution when compared to linear polymers of comparable molecular weight. All hyperbranched polymers in this study were found to be printable by DOD and CIJ at much higher concentrations than comparable linear polymers, without nozzle blockage or deterioration in print quality and as a consequence has the technical advantage of enabling the deposition of large volumes of functional polymeric materials in a single pass with the resultant increase in speed.

For both the low and medium branched samples, LB and MB, a reduction of the high molecular weight fraction and concomitant increase in the <500 kDa fraction was observed irrespective of polymer concentration with behaviour similar to that of linear polymer. However when the degree of branching is increased further with the HB sample, the molecular weight distribution is largely unaffected by the inkjet printing process apart from a small shaving of the highest molecular weight fractions, ca 10^7 kDa. This resistance to molecular degradation arises from the longest chain segment being much smaller, such that upon jetting the polymer rapidly retains its thermodynamically stable Gaussian coil conformation and the full force of the constrictional flow in the print head is not passed on to the polymer and degradation is supressed.

Acknowledgements

Joseph Wheeler would like to thank Domino UK Ltd for funding. This work was in part funded by the Engineering and Physical Sciences Research Council (EP/K039547/1). We also thank Dr.

Daniels Sells and the EPSRC National EPR Facility at Manchester for measurements. All data accompanying this publication are directly available within the paper and supplemental information.

Appendix A. Supplementary data

Supplementary data related to this article can be found at http://dx.doi.org/10.1016/j.polymdegradstab.2016.02.012

References

[1] H.M. Haverinen, R.A. Myllylä, G.E. Jabbour, Appl. Phys. Lett. 94 (2009) 073108.
[2] C. Zhang, K. Fang, Surf. Coatings Technol. 203 (2009) 2058–2063.
[3] R.E. Saunders, B. Derby, Int. Mater. Rev. 59 (2014) 430–448.
[4] K. Abe, K. Suzuki, D. Citterio, Anal. Chem. 80 (18) (2008) 6928–6934.
[5] E. Tekin, P.J. Smith, U.S. Schubert, Soft Matter 4 (2008) 703–713.
[6] S. Magdassi, The Chemistry of Inkjet Inks (Chapter 1), World Scientific Publishing, New York, 2010, pp. 6–15.
[7] J. Eggers, Z. Agnew, Math. Mech. 85 (6) (2005) 400–410.
[8] J.T. Kirk, G.E. Fridley, J.W. Chamberlain, E.D. Christensen, M. Hochberg, D.M. Ratner, Lab. Chip 11 (2011) 1372–1377.
[9] Z. Xiong, C. Liu, Org. Electron. 13 (2012) 1532–1540.
[10] S.D. Hoath, S. Jung, W. Hsiao, I.M. Hutchings, Org. Electron 13 (2012) 3259–3262.
[11] Y. Xu, I. Hennig, D. Freyberg, A.J. Strudwick, M.G. Schwab, T. Weitz, K.C. Cha, J. Power Sources 248 (2014) 483–488.
[12] T. Okamoto, T. Suzuki, N. Yamamoto, Nat. Biotechnol. 18 (2000) 438–441.
[13] D. Xu, V. Sanchez-Romaguera, S. Barbosa, W. Travis, J. de Wit, P. Swan, S.G. Yeates, J. Mater. Chem. 17 (2007) 4903–4907.
[14] S.D. Hoath, O.G. Harlen, I.M. Hutchings, J. Rheol. 56 (2012) 1109–1129.
[15] S.D. Hoath, D.C. Vadillo, O.G. Harlen, C. McIlroy, N.F. Morrison, W. Kai -Hsiao, T.R. Tuladhar, S. Jung, G.D. Martin, I.M. Hutchings, J. Newt. Fluid Mech. 205 (2014) 1–10.
[16] A. Keller, J. Odell, Nature 312 (1984) 98.
[17] A. Keller, J.A. Odell, Colloid. Polym. Sci. 263 (1985) 181–201.
[18] J.A. Odell, A. Keller, J. Polym. Sci. Part B Polym. Phys. 24 (1986) 1889–1916.
[19] A.J. Moller, J.A. Odell, A. Keller, J. Non-newton Fluid Mech. 30 (1988) 99–118.
[20] K. Al-Alamry, K. Nixon, R. Hind, J.A. Odel, S.G. Yeates, Macromol. Rapid Commun. 32 (3) (2011) 316–320.
[21] J.S.R. Wheeler, S.W. Reynolds, S. Lancaster, V. Sanchez-Romaguera, S.G. Yeates, Polym. Degrad. Stab. 105 (2014) 116–121.
[22] J. Wheeler, K. A-Alamry, S.W. Reynolds, S. Lancaster, N.M.P.S. Ricardo, S.G. Yeates, in: 2014 International Conference on Digital Printing Technologies 4, 2014, pp. 335–338.
[23] C. McIlroy, O.G. Harlan, N.F. Morrisson, J. Newt. Fluid Mech. 201 (2013) 17–28.
[24] M.G. McKeeb, S. Unala, G.L. Wilkesb, T.E. Long, Prog. Polym. Sci. 30 (2005) 507–539.
[25] B.I. Voit, A. Lederer, Chem. Rev. 109 (2009) 5924–5973.
[26] B.J. de Gans, L.J. Xue, U.S. Agarwal, U.S. Schubert, Macromol. Rapid Commun. 26 (4) (2004) 310–314.
[27] F. Isaure, P.A.G. Cormack, D.C. Sherrington, Macromolecules 37 (2004) 2096–2105.
[28] S. Camerlynck, P.A.G. Cormack, D.C. Sherrington, G. Saunders, J. Macromol. Sci. Phys. 44 (2005) 881–895.
[29] S.P. Gretton-Watson, E. Alpay, J.H.G. Steinke, J.S. Higgins, Ind. Eng. Chem. Res. 44 (2005) 8682–8693.
[30] C.J. Hawker, R. Lee, J.M. Frechet, J. Am. Chem. Soc. 113 (1991) 4583.
[31] B. Derby, N. Reis, MRS Bull. 28 (2003) 815–820.
[32] N. Reis, C. Ainsley, B. Derby, J. Appl. Phys. 97 (2005) 094903.
[33] R.D. Deegan, O. Bakajin, T.F. Dupont, G. Huber, S.R. Nagel, T.A. Witten, Nature 389 (1997) 827–829.
[34] K.S. Suslick, G.J. Price, Annu. Rev. Mater. Sci. 29 (1999) 295–326.
[35] B.E. Noltingk, E.A. Neppiras, Proc. Phys. Soc. Sect. B 63B (1950) 674.
[36] M.M. Caruso, D.A. Davis, Q. Shen, S.A. Odom, N.R. Sottos, S.R. White, J.S. Moore, Chem. Rev. 109 (11) (2009) 5755–5798.
[37] O. Altintas, M. Abbasi, K. Riazi, A.S. Goldmann, N. Dingenouts, M. Wilhelm, C. Barner-Kowollik, Polym. Chem. 5 (2014) 5009.
[38] C.E. Diesendruck, G.I. Peterson, H.J. Kulik, J.A. Kaitz, B.D. Mar, P.A. May, S.R. White, T.J. Martınez, A.J. Boydston, J.S. Moore, Nat. Chem. 6 (2014), 632–628.